Non-algebraic domain growth for phase ordering dynamics in a random field

1993 J. Phys. A: Math. Gen. 26 2777

(http://iopscience.iop.org/0305-4470/26/12/018)

J. Phys. A: Math. Gen. 26 (1993) 2089–2101. Printed in the UK

Non-algebraic domain growth for phase ordering dynamics in a random field

Sanjay Puri and Nita Parekh

School of Physical Sciences, Jawaharlal Nehru University, New Delhi—110067, India

Received 11 May 1992

Abstract. We present the third (and final) paper in our three-stage numerical exposition of the effects of quenched disorder on phase ordering dynamics. In this paper, we study the effects of random fields on domain growth. Our numerical results indicate that the domain growth law is logarithmic for both the cases with non-conserved and conserved order parameter. This is compatible with theoretical expectations. We also study the dynamical scaling of the structure factor for both the non-conserved and conserved cases.

1. Introduction

There has been much interest in the study of phase ordering dynamics, namely the dynamics of domain growth in two-phase mixtures which have been rendered thermodynamically unstable by quenching below the critical coexistence temperature T_c [1]. Most of the numerical and theoretical attention has been focused on pure and isotropic systems, which have already been the subject of substantial controversy. Now, it is well established that domain growth in pure and isotropic systems is characterized by a unique, time-dependent length scale $R(t)$ (where t is the time). This length scale has a power-law dependence on time, namely $R(t) \approx t^{\phi}$, where ϕ is called the growth exponent. For the case with non-conserved order parameter (e.g. ordering of a ferromagnet), $\phi = \frac{1}{2}$ [1]. For the case with conserved order parameter but no hydrodynamic effects (e.g. segregation of a binary alloy), $\phi = \frac{1}{3}$ [1]. For the case with conserved order parameter and where hydrodynamic effects are relevant (e.g. segregation of a binary fluid), recent numerical results [2] demonstrate conclusively that $\phi = 1$, a result that was theoretically proposed by Siggia [3] some time ago.

Naturally, experimental systems are neither pure nor isotropic. Impurities in binary mixtures (e.g. mobile or immobile vacancies [4], random fields [5]) act as trapping centres for growing domains and alter the growth laws mentioned above. Anisotropy in binary mixtures is introduced by external effects (e.g. gravitational fields [6], surfaces [7]) or internal effects (e.g. strain [8]) and can dramatically alter the dynamics of phase ordering in affected systems. Any realistic simulation (or theory, for that matter) of an experimental situation must account for the above effects. In an attempt to address some of these realistic effects, we have initiated a three-stage study of the effects of disorder on the dynamics of phase ordering. There have been a number of Monte Carlo (MC) simulations of these effects [9–12]. Unfortunately, these have not been conclusive in fixing either the domain growth law or the nature of dynamical scaling of the structure factor. (An exception is the recent MC study of random magnets by Bray and Humayun [9]). We have approached this problem using coarse-grained cell

0305-4470/93/122777+13$07.50

dynamical system (CDS) models [13], which have had considerable success in elaborating the nature of domain growth in pure and isotropic systems. In the first stage of our present exposition (referred to as I), we considered the slowing down of ordering in random magnets (i.e. the case with non-conserved order parameter) [14]. In the second stage of our exposition (referred to as II), we reported on non-algebraic domain growth in binary alloys [15]. This is the third and final paper in our exposition. In this paper, we present comprehensive results (from CDS models) for domain growth in Ising-like systems with random fields. We will consider the cases with both non-conserved and conserved order parameter.

This paper is organized in the following fashion. In section 2 we describe the CDS models used in this study. In section 3 we describe our results for the case with non-conserved order parameter. Section 4 reports our results for the case with conserved order parameter. In section 5 we end with a summary and discussion.

2. Modelling the presence of random fields

The starting point of our modelling is the time-dependent Ginzburg–Landau (TDGL) equation which describes the temporal evolution of a system described by a non-conserved order parameter (e.g. a coarse-grained version of the Ising model with Gauber kinetics [16]),

$$\frac{\partial\psi(\boldsymbol{r},t)}{\partial t}=-L\frac{\delta H[\psi(\boldsymbol{r},t)]}{\delta\psi(\boldsymbol{r},t)}+\sigma(\boldsymbol{r},t). \tag{2.1}$$

In (2.1), $\psi(\boldsymbol{r},t)$ is the scalar order parameter at point $\boldsymbol{r}$ and time t; and L is a phenomenological parameter. For the Ising model in an external space-dependent field, the coarse-grained free-energy functional $H[\psi(\boldsymbol{r},t)]$ in (2.1) is usually taken to be of the ϕ^4 form, namely,

$$H[\psi(\boldsymbol{r},t)]=\int \mathrm{d}\boldsymbol{r}\left[-\frac{\tau}{2}\psi(\boldsymbol{r},t)^2+\frac{g}{4}\psi(\boldsymbol{r},t)^4+\frac{K}{2}(\nabla\psi(\boldsymbol{r},t))^2+h(\boldsymbol{r})\psi(\boldsymbol{r},t)\right] \tag{2.2}$$

where τ, g and K are phenomenological constants which respectively measure the temperature T ($\tau\sim(T_c-T)$, where T_c is the critical temperature); the coupling constant; and the interfacial energy. The external field $h(\boldsymbol{r})$ couples linearly with the order parameter [17]. The Gaussian white noise $\sigma(\boldsymbol{r},t)$ satisfies the fluctuation–dissipation relation

$$\langle\sigma(\boldsymbol{r},t)\sigma(\boldsymbol{r}',t')\rangle=2TL\delta(\boldsymbol{r}-\boldsymbol{r}')\delta(t-t') \tag{2.3}$$

where we have set the Boltzmann constant to unity. The TDGL equation corresponding to the free-energy functional (2.2) is then

$$\frac{\partial\psi(\boldsymbol{r},t)}{\partial t}=L[\tau\psi(\boldsymbol{r},t)-g\psi(\boldsymbol{r},t)^3+K\nabla^2\psi(\boldsymbol{r},t)+h(\boldsymbol{r})]+\sigma(\boldsymbol{r},t). \tag{2.4}$$

The corresponding partial differential equation for the temporal evolution of a binary alloy with a space-dependent external field is

$$\frac{\partial\psi(\boldsymbol{r},t)}{\partial t}=-L\nabla^2[\tau\psi(\boldsymbol{r},t)-g\psi(\boldsymbol{r},t)^3+K\nabla^2\psi(\boldsymbol{r},t)+h(\boldsymbol{r})]+f(\boldsymbol{r},t). \tag{2.5}$$

Equation (2.5) is a simple generalization of the Cahn–Hilliard–Cook equation [18], which describes the evolution of a binary alloy undergoing phase segregation. This phenomenological equation can be motivated [19] by applying the master equation approach [16] to the random field Ising model (RFIM) with Kawasaki kinetics, which is the appropriate microscopic model for this case. In (2.5), the noise $f(\boldsymbol{r}, t)$ is Gaussian with mean zero and satisfies the fluctuation–dissipation relation

$$\langle f(\boldsymbol{r}, t) f(\boldsymbol{r}', t') \rangle = -2TL\nabla^2 \delta(\boldsymbol{r}-\boldsymbol{r})\delta(t-t'). \tag{2.6}$$

In papers I and II, we have rescaled (2.4) and (2.5) and cast them in a dimensionless form. We do not repeat this rescaling here but rather just write down the corresponding dimensionless forms. For the non-conserved case, we have [14]

$$\frac{\partial \psi(\boldsymbol{r}, t)}{\partial t} = \psi(\boldsymbol{r}, t) - \psi(\boldsymbol{r}, t)^3 + \nabla^2 \psi(\boldsymbol{r}, t) + \bar{h}(\boldsymbol{r}) + \sqrt{\varepsilon}\mu(\boldsymbol{r}, t) \tag{2.7}$$

where ψ, $\boldsymbol{r}$ and t are now all dimensionless; and

$$\begin{aligned} \bar{h}(\boldsymbol{r}) &= \sqrt{(g/\tau^3)}\, h(\boldsymbol{r}) \\ \varepsilon &= \frac{2gT}{\tau^2}\left(\frac{\tau}{k}\right)^{d/2} \end{aligned} \tag{2.8}$$

d being the dimensionality. For the conserved case, we have [15]

$$\frac{\partial \psi(\boldsymbol{r}, t)}{\partial t} = -\nabla^2[\psi(\boldsymbol{r}, t) - \psi(\boldsymbol{r}, t)^3 + \nabla^2 \psi(\boldsymbol{r}, t) + \bar{h}(\boldsymbol{r})] + \sqrt{\varepsilon}\mu(\boldsymbol{r}, t) \tag{2.9}$$

where (again) the variables are now dimensionless; and

$$\begin{aligned} \bar{h}(\boldsymbol{r}) &= K\sqrt{(g/\tau^5)}h(\boldsymbol{r}) \\ \varepsilon &= \frac{2gT}{\tau^2}\left(\frac{\tau}{k}\right)^{d/2}. \end{aligned} \tag{2.10}$$

Equations (2.7) and (2.9) are used to construct computationally efficient CDS models, as is already discussed extensively in the literature [13–15]. We do not reiterate the procedure here but merely write down the corresponding CDS models. For the non-conserved case, we have

$$\psi(\boldsymbol{r}, t+1) = f_A(\psi(\boldsymbol{r}, t)) + D\Delta_D \psi(\boldsymbol{r}, t) + H(\boldsymbol{r}) + B\mu(\boldsymbol{r}, t) \tag{2.11}$$

where the time t is incremented in discrete steps; and the function $f_A(x)$ is the piecewise linear function

$$\begin{aligned} f_A &= Ax \qquad |x| \leqslant 1/A \\ &= \operatorname{sgn}(x) \qquad |x| > 1/A \end{aligned} \tag{2.12}$$

A being a parameter (>1). This function has an unstable fixed point at $x=0$ (corresponding to the homogeneous state) and two symmetrically placed stable fixed points at $x=\pm 1$ (corresponding to the stable 'spin-up' and 'spin-down' states). In (2.12), D is also a parameter and Δ_D is the isotropically discretized Laplacian operator at a point. We will take $H(\boldsymbol{r})$ to be a random field with amplitude C, where C is the third parameter in our model. Finally, there is a fourth parameter B, which measures the strength of the random noise.

For the case with conserved order parameter, we desire to construct the CDS model which mimicks the dynamics of (2.9). In the continuum case, the partial differential

equation which describes the case with conserved order parameter is naively obtained by appending an $(-\nabla^2)$ operator to the chemical potential in the TDGL equation. The required CDS model for the conserved dynamics is obtained analogously [13] from (2.11) as

$$\psi(\boldsymbol{r}, t+1) = \psi(\boldsymbol{r}, t) - \Delta_D[f_A(\psi(\boldsymbol{r}, t)) - \psi(\boldsymbol{r}, t) + D\Delta_D\psi(\boldsymbol{r}, t) + H(\boldsymbol{r})] + B\theta(\boldsymbol{r}, t) \qquad (2.13)$$

where (again) the time t is incremented in discrete time steps. The CDS models described by (2.11) and (2.13) have been used to obtain the two-dimensional results described in sections 3 and 4.

There are four parameters in our models, namely the constants A and D; the amplitude of the random field C; and the noise amplitude B. The choice of parameters is dictated by the requirements that the schemes be numerically stable; and the results obtained be reasonable [13]. We use the parameter values $A = 1.3$ and $D = 0.125$, which have proved appropriate for the case without disorder [13]. Essentially, the values of A and D affect only the width of the interface between domains and not the bulk of the domains. Asymptotically, the width of the interface (which is constant in time) is an irrelevant variable compared to the characteristic domain size (which grows in time). Thus, the only effect of the interface width is to introduce non-universal features in the scaled structure factors at early times. Asymptotically, scaled structure factors are independent of the interface width and, consequently, independent of the values of A and D. This has been confirmed for the case with disorder, though we do not present detailed results here. The asymptotic results presented below are independent of the values of A and D over a broad range of values.

Let us next discuss the role played by the random field. Results described here are for the case where $H(\boldsymbol{r})$ is uniformly and randomly distributed between $-C$ and $+C$, where we will specify the different values of C subsequently. For completeness, we have also performed simulations in which the random field is Gaussian distributed. The results are identical to those presented here and, hence, we do not present the results for Gaussian distributed random fields.

Finally, the choice of the noise amplitude raises some important questions. In the case of pure systems, the presence of noise only affects the smoothness of the interface of the domains. With the passage of time, the interface thickness (or raggedness) is irrelevant in comparison to the characteristic domain size. Therefore, for pure systems, noise is an irrelevant variable asymptotically and this has been demonstrated numerically [13]. However, domain growth in disordered systems is driven by the thermally assisted hopping of energy barriers created by the disorder traps. In the absence of thermal noise, the system is plagued by freezing effects and it is hard to get domain growth over extended time regimes. Thus, we choose a non-zero noise amplitude ($B = 0.3$) for our simulations. Numerically, we choose noise to be uniformly and randomly distributed between -0.3 and 0.3 for the non-conserved case. For the conserved case, we should caution the reader that the noise term has to be chosen more carefully as the noise must satisfy a more complicated fluctuation-dissipation relation, namely equation (2.6). Thus, for the conserved case, the noise is chosen to be of the form $\theta(\boldsymbol{r}, t) \equiv \nabla_D \mu(\boldsymbol{r}, t)$ [13], ∇_D is the symmetrically discretized divergence operator at a point; and $\mu(\boldsymbol{r}, t)$ is a vector field (with d components), whose elements are uniformly and randomly distributed between -0.3 and 0.3. (Again, we have also done simulations with Gaussian distributed noise. The results are identical to those presented here. Furthermore, different noise amplitudes give similar growth to that described here. Thus, we do not present these results here.)

3. Numerical results for the case with non-conserved order parameter

We have implemented the scheme (2.11) on a 128×128 lattice with periodic boundary conditions. The quantity usually calculated is the time-dependent structure factor, which is defined as

$$S(k, t) = [\langle \psi(k, t)(\psi(k, t)^*) \rangle] \tag{3.1}$$

where $\psi(k, t)$ is the Fourier transform of $\psi(r, t)$ on the discrete lattice; the angular brackets denote an averaging over different initial conditions; the square brackets denote an averaging over different disorder configurations; and the * denotes complex conjugation. The wavevector k take up the discrete values $2\pi(k_x, k_y)/128$, where k_x and k_y range from 1 to 128. For each fixed configuration of disorder, we obtain structure factors as averages over 20 different initial conditions. Then, we average over (typically) 20 different configurations of the random field. The time-dependent structure factors are circularly averaged to give the scalar function $S(k, t)$, which will be shown in subsequent figures. The characteristic domain size $\langle R \rangle(t)$, is defined as the reciprocal of the first moment of the scalarized structure factor, i.e. $\langle R \rangle(t) = \langle k \rangle(t)^{-1}$, where $\langle k \rangle(t)$ is defined as

$$\langle k \rangle(t) = \frac{\int_0^{k_m} \mathrm{d}k\, kS(k, t)}{\int_0^{k_m} \mathrm{d}k\, S(k, t)} \tag{3.2}$$

where k_m is the magnitude of the largest wavevector we consider. The results presented here are for k_m equal to half the magnitude of the largest wavevector lying in the Brillouin zone of the lattice. The characteristic length scale thus measured is in units of the lattice spacing.

Figure 1 shows the characteristic length scale $\langle R \rangle(t)$ as a function of time t for different amplitudes of the random field (as indicated). In this figure, we have plotted $\langle R \rangle(t)^2$ against t as it is known that domain growth for the TDGL without a random

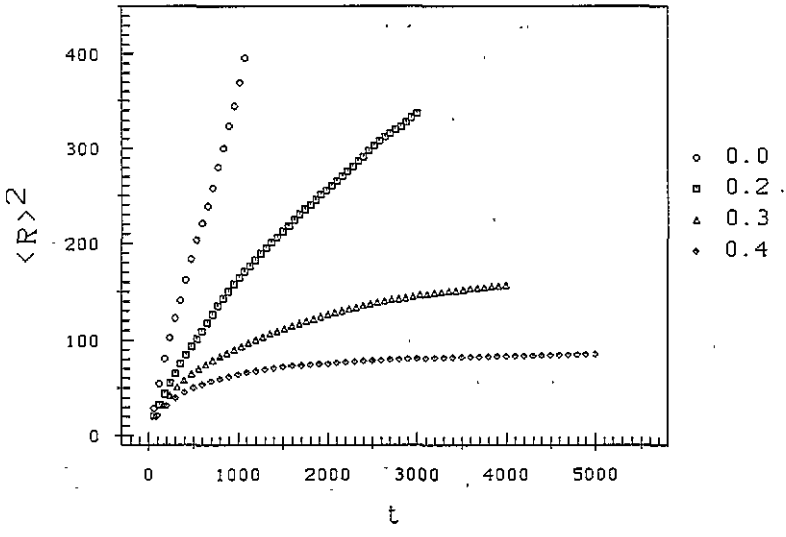

Figure 1. Plot of $\langle R \rangle(t)^2$ against t for the non-conserved case, where $\langle R \rangle(t)$ is the characteristic domain size at time t. Data is presented for disorder amplitudes $C = 0.0$ (the pure case, marked by circles); and $C = 0.2$, 0.3, 0.4 (marked by the symbols indicated).

field obeys the Lifshitz–Cahn–Allen (LCA) growth law $\langle R\rangle(t) \approx t^{1/2}$. In figure 1, data for the pure system is denoted by circles and is seen to obey the LCA growth law. For very early times, data for the disordered case also obeys the LCA growth law (not evident on the scale of figure 1) but there is a rapid crossover to a non-LCA growth regime. The crossover is faster for higher amplitudes of the random field. This is qualitatively similar to the crossover to non-algebraic domain growth random exchange magnets [14]. Villain and Grinstein and Fernandez [20] have theoretically argued that the asymptotic growth law is logarithmic in time. In figure 2, we plot $\langle R\rangle(t)$ against ln t and find that the data for the TDGL equation with non-zero random field shows logarithmic growth over extended periods of time. Unfortunately, freezing affects our data at later times for the stronger values of random field amplitude. Thus, for $C = 0.3$ (or $C = 0.4$), freezing results in a deviation from the logarithmic growth law at approximately $t = 2700$ (or $t = 1630$). This is consistent with the results of Oguz *et al* [12] obtained by the direct integration of the TDGL equation with a random field in two dimensions.

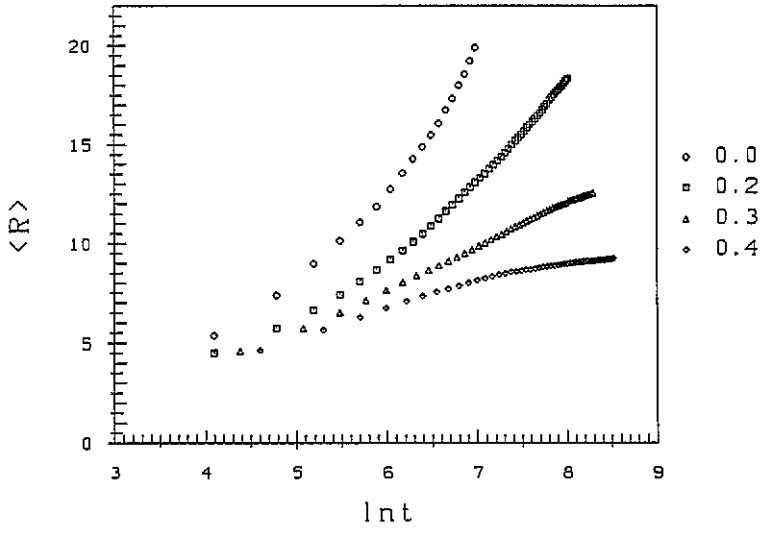

Figure 2. Plot of $\langle R\rangle(t)$ against ln t for the data from figure 1. Different disorder amplitudes are denoted by the same symbols as in figure 1.

Let us next consider the dynamical scaling of the structure factor. The existence of a unique length scale ensures that the scalarized structure factor has the dynamical scaling form [21]

$$S(k, t) = \langle k\rangle(t)^{-d} F(k/\langle k\rangle(t)) \tag{3.3}$$

where $F(x)$ is the so-called master function. We have confirmed the validity of dynamical scaling by superimposing (not shown here) data for $S(k, t)\langle k\rangle(t)^2$ against $k/\langle k\rangle(t)$ from different times for the different disorder amplitudes shown in figure 1. Data for different times collapses well onto a single master curve (as expected). (At stronger fields than those shown here, there is some evidence for a breakdown in the scaling behaviour, as expected by Grant and Gunton [22] due to the absence of long-range order for the RFIM in two dimensions. However, this needs to be carefully investigated and we are presently performing longer simulations on larger systems so

as to clarify this). In figure 3(a), we test for what we refer to as 'superscaling', namely we superimpose $S(k, t)\langle k\rangle(t)^2$ against $k/\langle k\rangle(t)$ for different disorder amplitudes. Data is from different times $t = 1000$ (for $C = 0.0$, the pure case); and $t = 3000$ (for $C = 0.2$, 0.3, 0.4). The excellent collapse of the data indicates that superscaling holds good, i.e. the form of the master function is independent of the amplitude of the random field (for the range of disorder amplitudes considered here) and is the same as that for the pure case. To confirm that superscaling holds good in the tail region also, figure 3(b) shows the data from figure 3(a) on a semi-logarithmic scale, namely we plot $\ln(S(k, t)\langle k\rangle(t)^2)$ against $k/\langle k\rangle(t)$. We have earlier reported similar superscaling of the

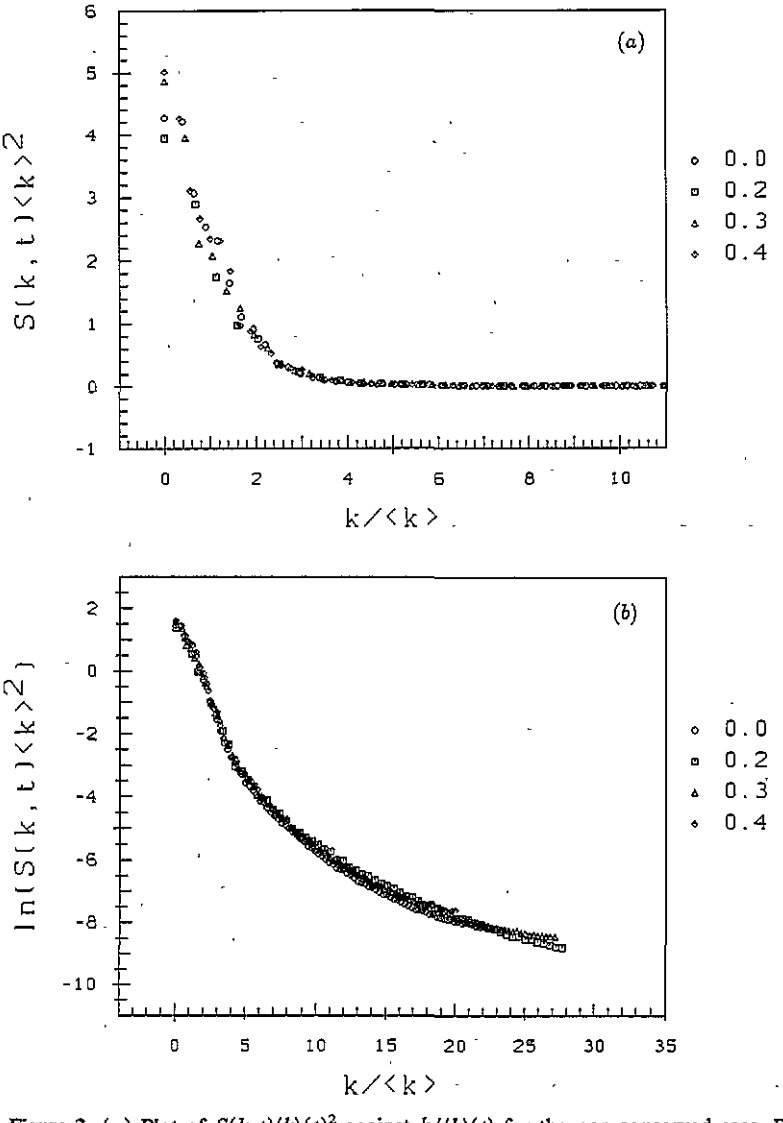

Figure 3. (a) Plot of $S(k, t)\langle k\rangle(t)^2$ against $k/\langle k\rangle(t)$ for the non-conserved case. Data is for disorder amplitudes $C = 0.0$ at $t = 1000$ (the pure case, marked by circles); and $C = 0.2$, 0.3, 0.4 at $t = 3000$ (marked by the symbols indicated). (b) Plot of $\ln(S(k, t)\langle k\rangle(t)^2)$ against $k/\langle k\rangle(t)$ for the data from figure 3(a). Symbols used have the same meaning as in figure 3(a).

structure factor in our simulations of random magnets [14] and binary alloys [15] with quenched disorder in the parameters τ and g in (2.2).

4. Numerical results for the case with conserved order parameter

We have also implemented the scheme (2.13) on a 128×128 lattice with periodic boundary conditions. The quantities calculated; the statistics; and averaging procedures are identical to those described in the previous section. Thus, we directly move on to a description of our numerical results.

In figure 4, we plot $\langle R \rangle(t)^3$ against t for the pure case ($C = 0.0$) and various values of disorder ($C = 0.2$, 0.3, 0.4 and 0.5, marked by the symbols indicated). The growth law for the pure case is the well known Lifshitz–Slyozov (LS) law ($\langle R \rangle(t) \approx t^{1/3}$) and this appears as a straight line (marked by circles) in figure 4. For early times, even the data for the disordered case obeys the LS law as the domains are too small to be affected by the disorder. However, there is a rapid crossover to a non-LS growth regime and (as before) the crossover is earlier for higher disorder amplitudes. Based on the theoretical predictions of Villain and Grinstein and Fernandez [20], we expect the asymptotic growth law to be logarithmic in this case also, as the arguments for logarithmic growth are independent of whether or not the order parameter is conserved. In figure 5, we plot $\langle R \rangle(t)$ against $\ln t$ and find that we have clear evidence of an extended logarithmic growth regime for all non-zero values of disorder amplitude. Some effects of freezing are seen at late times for $C = 0.5$ but they are not so pronounced.

Next, we consider the dynamical scaling of the structure factor. Figure 6(a) superimposes data for $S(k, t)\langle k \rangle(t)^2$ against $k/\langle k \rangle(t)$ from times $t = 4000$, 6000, 8000 and 10 000 (marked by the symbols indicated). The disorder amplitude is $C = 0.2$. The excellent data collapse indicates that dynamical scaling holds good in this case. In figure 6(b), we show a similar plot for $C = 0.4$. In this case, the dynamical scaling

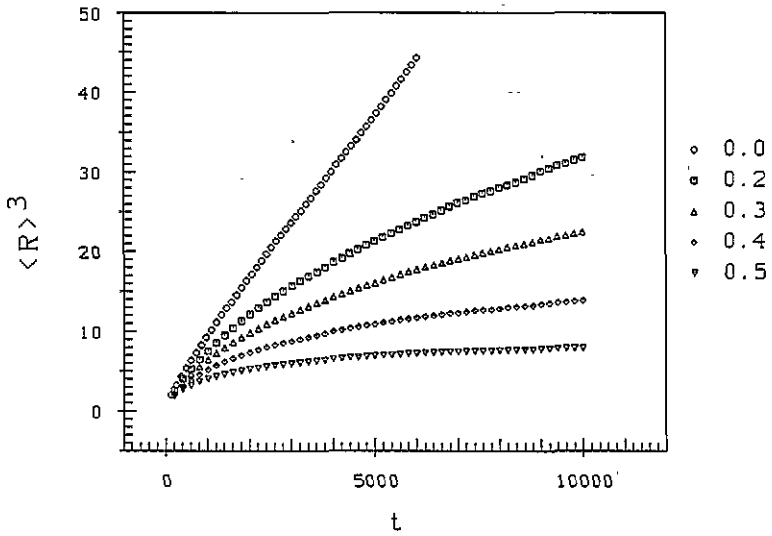

Figure 4. Plot of $\langle R \rangle(t)^3$ against t for the conserved case, where $\langle R \rangle(t)$ is the characteristic domain size at time t. Data is presented for disorder amplitudes $C = 0.0$ (the pure case, marked by circles); and $C = 0.2$, 0.3, 0.4 (marked by the symbols indicated).

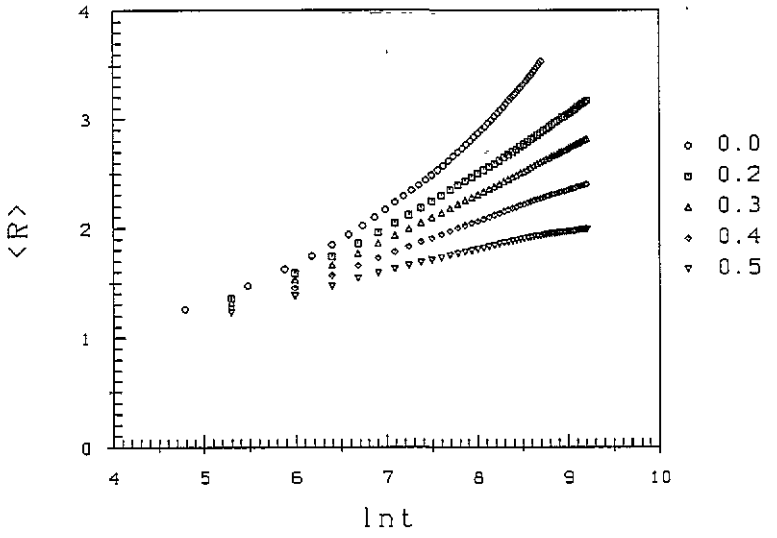

Figure 5. Plot of $\langle R\rangle(t)$ against ln t for the data from figure 4. Different disorder amplitudes are denoted by the same symbols as in figure 4.

does not appear to hold and there is a systematic shift (towards an asymmetric form) in the universal function at later times. The effect is even more pronounced for $C=0.5$, data for which we do not present here. Figure 7(a) shows that superuniversal scaling does not hold either, even for disorder amplitudes at which scaling holds good (e.g. $C=0.2$). In figure 7(a) we superimpose $S(k,t)\langle k\rangle(t)^2$ against $k/\langle k\rangle(t)$ for $t=10\,000$ and disorder amplitudes $C=0.0$, 0.2 and 0.4 (marked by the symbols shown). The 'master function' for $C=0.4$ (though the term is a bit misleading as there is no scaling) is quite different from the master function for the pure case, as is expected. However, even for $C=0.2$ (where scaling does hold good over the timescales of observation), the master function has a lower peak and is more asymmetric than that for the pure case. This is in contrast to our observation in the non-conserved case where domain growth which obeyed dynamical scaling also showed superscaling, namely no dependence of the master function on the disorder amplitude. The difference in the tails of the master functions is highlighted in figure 7(b), where we plot $\ln(S(k,t)\langle k\rangle(t)^2)$ against $k/\langle k\rangle(t)$.

5. Summary and discussion

This was the third (and final) paper of a three-stage exposition. In our first two papers ([14](I) and [15](II)), we presented detailed numerical results for CDS models which mimicked domain growth in random magnets and binary alloys with quenched disorder (e.g. immobile vacancies). In this paper, we have presented extensive numerical results from a CDS study of the effect of random fields on the dynamics of phase ordering in the cases of both non-conserved and conserved order parameter. We initiated this study because we felt that coarse-grained, computationally efficient models would help elaborate the nature of domain growth in disordered systems. Microscopic Monte Carlo (MC) models have been somewhat inconclusive in this regard. At this stage, it

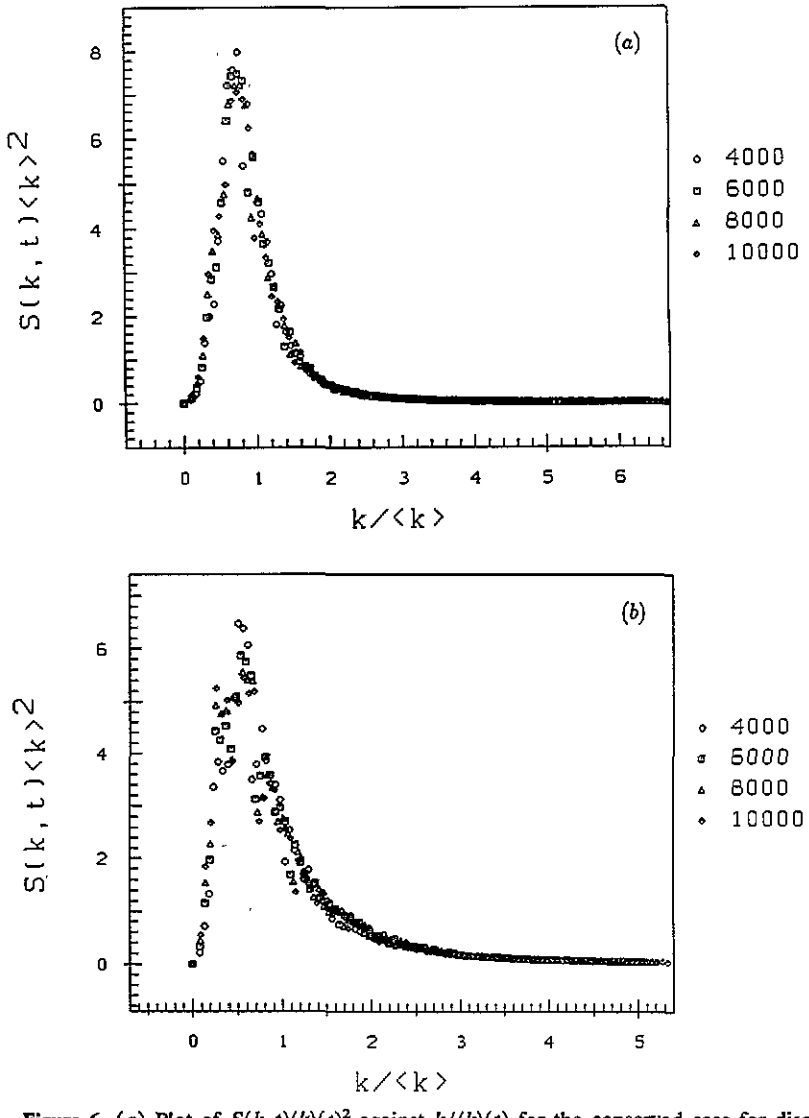

Figure 6. (*a*) Plot of $S(k,t)\langle k\rangle(t)^2$ against $k/\langle k\rangle(t)$ for the conserved case for disorder amplitude $C=0.2$. Data is from times $t=4000$, 6000, 8000 and 10 000 (marked by the symbols indicated). (*b*) Plot of $S(k,t)\langle k\rangle(t)^2$ against $k/\langle k\rangle(t)$ for the conserved case for disorder amplitude $C=0.4$. Data is from times $t=4000$, 6000, 8000 and 10 000 (marked by the symbols indicated).

is natural to question what degree of success we have enjoyed in achieving our stated goal.

In paper I, we studied the CDS equivalent of a two-dimensional TDGL model with disorder in the values of the parameters τ and g in (2.2). We made two important observations regarding this model. Firstly, we found that the domain growth law was compatible with $\langle R\rangle(t)\approx(\ln t)^4$ (the so-called Huse–Henley law [23]) over a limited range of disorder amplitudes and times. Unfortunately, there were a number of factors (e.g., finite-size effects, freezing) which resulted in our data not being very clear with regard to the asymptotic growth law. Nevertheless, our results were a substantial

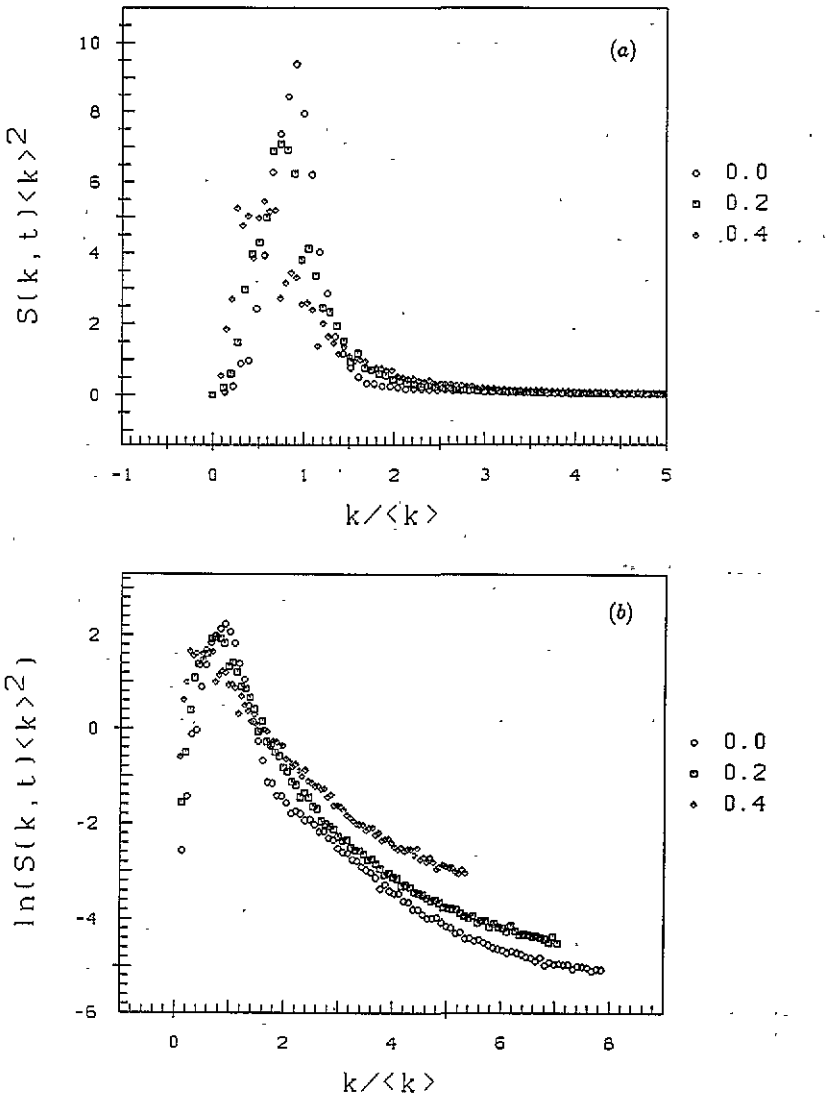

Figure 7. (*a*) Plot of $S(k,t)\langle k\rangle(t)^2$ against $k/\langle k\rangle(t)$ for the non-conserved case. Data is for disorder amplitudes $C=0.0$ at $t=1000$ (the pure case, marked by circles); and $C=0.0$, 0.2, 0.4 at $t=10\,000$ (marked by the symbols indicated). (*b*) Plot of $\ln(S(k,t)\langle k\rangle(t)^2)$ against $k/\langle k\rangle(t)$ for the data from figure 7(*a*). Symbols used have the same meaning as in figure 7(*a*).

improvement on existing MC results [9]. Our second important observation was that the scaled structure factor showed a superuniversal scaling, namely the structure factor showed dynamical scaling for all values of disorder and the universal function obtained thus was independent of the disorder amplitude (even in the tail). This result was quite unambiguous and should be verifiable experimentally.

In paper II, we presented results for the conserved equivalent of the model in paper I. For the conserved case, we were not able to clearly establish a domain growth law, though it is our expectation (theoretically) that it should be the same as in the non-conserved case. Of course, it is possible that this was because our simulation did

not access the true asymptotic regime. However, we were again able to clearly establish the superuniversal scaling of the structure factor, a fact that should emerge in experiments also. To the best of our knowledge, there are no MC studies of the conserved case with disorder.

In this paper, (which we refer to as III), we have presented detailed numerical results for domain growth in the presence of random fields. For the non-conserved case, we showed that $\langle R\rangle(t) \approx \ln t$ over extended periods of time, though freezing effects do slow down the growth at later times. This was in conformity with the theoretical predictions of Villain and Grinstein and Fernandez [20], and the numerical results of Oguz *et al* [12]. For the disorder amplitudes presented here, the structure factors for different amplitudes of disorder obeyed dynamical scaling and the universal functions obtained thus were independent of the disorder amplitudes, i.e. we observed superuniversal scaling. For larger amplitudes of disorder, it seems that dynamical scaling might break down but this needs to be investigated further. For the conserved case, we were again able to demonstrate that $\langle R\rangle(t) \approx \ln t$ over extended periods of time. In this case, we did see a clear breakdown of dynamical scaling at high amplitudes of disorder. Further, even at lower amplitudes of disorder (where dynamical scaling holds good over the timescales of observation), superuniversal scaling did not hold and the master function appears to become progressively more asymmetric as the amplitude of disorder is increased.

It is our belief that papers I to III constitute the most detailed investigation (to date) of the effect of quenched disorder on domain growth. Our study has been greatly facilitated by the use of computationally efficient CDS models and we believe that these constitute the best prospect for further studies of the effects of disorder on phase ordering dynamics.

Acknowledgments

The authors are grateful to D Chowdhury for collaborating with them on the earlier parts of this problem. They are also grateful to him for many useful discussions and a critical reading of this manuscript. SP would like to thank A Bray for a number of insightful comments and discussions. Finally, SP is highly grateful to K Binder for his warm hospitality at Mainz, where part of the numerical computations described in the text were performed. One of the authors, NP, would like to thank CSIR, India for its financial support.

References

[1] For reviews see Gunton J D, San Miguel M and Sahni P S 1983 *Phase Transitions and Critical Phenomena* (vol 8) ed C Domb and J L Lebowitz (New York: Academic Press) p 267
Binder K 1987 *Rep. Prog. Phys.* **50** 783
Furukawa H 1985 *Adv. Phys.* **34** 703
Komura S 1988 *Phase Transitions* **12** 3
Komur S and Furukawa (eds) 1988 *Dynamics of Ordering Processes in Condensed Matter* (New York: Plenum)
Grant M *Int. J. Mod. Phys.* B in press
[2] Puri S and Dunweg B *Phys. Rev.* A (Rapid Communication) to appear
Koga T and Kawasaki K 1991 *Phys. Rev.* A **44** R817
[3] Siggia E D 1979 *Phys. Rev.* A **20** 595

[4] Flynn C P 1972 *Point Defects and Diffusion* (Oxford: Clarendon)
[5] For recent reviews see Nattermann T and Villain J 1988 *Phase Transitions* **11** 5
Nattermann T and Rujan P 1989 *Int. J. Mod. Phys.* B **11** 1597
[6] Kitahara K, Oono Y and Jasnow D 1988 *Mod. Phys. Lett.* B **2** 765
Puri S, Binder K and Dattagupta S *Phys. Rev.* A submitted
Puri S, Parekh N and Dattagupta S *Phys. Rev. Lett.* submitted
[7] Binder K and Frisch H L *Z. Phys.* B to appear
Puri S and Binder K *Phys. Rev.* A. submitted
[8] Onuki A 1991 *Phys. Rev.* B **43** 13649; 1991 *J. Phys. Soc. Japan* **60** 1; 1991 *J. Phys. Soc. Japan* **60** 345
[9] For Monte Carlo studies of the non-conserved case with quenched disorder see Grest G S and Srolovitz D J 1985 *Phys. Rev.* B **32** 3014
Chowdhury D, Grant M and Gunton J D 1987 *Phys. Rev.* B **35** 6792
Chowdhury D and Kumar S 1987 *J. Stat. Phys.* **49** 855
Oh J H and Choi D I 1986 *Phys. Rev.* B **33** 3448
Chowdhury D 1990 *J. Physique* **51** 2681
Bray A J and Humayun K 1991 *J. Phys. A: Math. Gen.* **24** L1185
[10] For Monte Carlo studies of the non-conserved case with annealed disorder see Srolovitz D J and Hassold G N 1987 *Phys. Rev.* B **35** 6902
Mouritsen O G and Shah P J 1989 *Phys. Rev.* B **40** 11445
Shah P J and Mouritsen O G 1990 *Phys. Rev.* B **41** 7003
[11] For Monte Carlo studies of the non-conserved case with random fields see
Chowdhury D and Stauffer D 1985 *Z. Phys.* B **60** 249
Pytte E and Fernandez J F 1985 *Phys. Rev.* B **31** 616
Gawlinski E T, Kumar S, Grant M, Gunton J D and Kaski K 1985 *Phys. Rev.* B **32** 1575
Anderson S R 1987 *Phys. Rev.* B **36** 8435
[12] For a simulation of a coarse-grained model of the non-conserved case with random fields see Oguz E, Chakrabarti A, Toral R and Gunton J D 1990 *Phys. Rev.* B **42** 704
[13] Oono Y and Puri S 1987 *Phys. Rev. Lett.* **58** 836; 1988 *Phys. Rev.* A **38** 434
Puri S and Oono Y 1988 *Phys. Rev.* A **38** 1542; 1988 *J. Phys. A: Math. Gen.* **21** L755
Puri S 1988 *Phys. Lett.* **134A** 205
[14] Puri S, Chowdhury D and Parekh N 1991 *J. Phys. A: Math. Gen.* **24** L1087
[15] Puri S and Parekh N *J. Phys. A: Math. Gen.* to appear in
[16] Binder K 1974 *Z. Phys.* B **267** 313 and references therein
[17] Grinstein G, Ma S K and Mazenko G F 1977 *Phys. Rev.* B **15** 258
Ma S K 1982 *Modern Theory of Critical Phenomena* (California: Addison-Wesley)
[18] Cahn J W and Hilliard J E 1958 *J. Chem. Phys.* **28** 258; 1959 *J. Chem. Phys.* 688
Cahn J W 1969 *Acta. Met.* **9** 795
Cook H E 1970 *Acta. Met.* **18** 297
[19] Puri S unpublished
[20] Villain J 1984 *Phys. Rev. Lett.* **52** 1543
Grinstein G and Fernandez J F 1984 *Phys. Rev.* B **29** 6389
[21] Binder K and Stauffer D 1974 *Phys. Rev. Lett.* **33** 1006; 1976 *Z. Phys.* B **24** 407
[22] Grant M and Gunton J D 1984 *Phys. Rev.* B **29** 6266; 1987 *Phys. Rev.* B **35** 4922
[23] Huse D A and Henley C L 1985 *Phys. Rev. Lett.* **54** 2708